2021 American Control Conference (ACC)
New Orleans, USA, May 25-28, 2021

Al-Darabsah, I., Janaideh, M. A., & Campbell, S. A. (2021). Stability of Connected Autonomous Vehicle Networks with Commensurate Time Delays. 2021 American Control Conference (ACC), 3308–3313. https://doi.org/10.23919/ACC50511.2021.9482938

Stability of Connected Autonomous Vehicle Networks with Commensurate Time Delays

Isam Al-Darabsah, Mohammad Al Janaideh, and Sue Ann Campbell

Abstract— **In this paper, we study the stability of Connected Autonomous Vehicle Networks (CAVN) with commensurate time delays under the assumption that communication time delays increase as the distance between the vehicles increases. Two delays are said to be commensurate if their ratio is a rational number. We characterize the maximum range of delay where the system becomes plant stable and carry out string stability analysis. We provide numerical simulation and observe that the stability region in the control gains plane decreases as when commensurate time delays increase.**

I. Introduction

Connected Autonomous Vehicle Network (CAVN) is new technology that communicates and controls the speed and position of autonomous vehicles through a wireless exchange of information between these vehicles within a network [1]. This new technology represents an emerging cyber-physical system (networking, computation, and physical processes) with significant potential to enhance vehicle safety, ease traffic congestion and positively impact the environment through autonomous platoon control. The cyber component of such a system incorporates a vehicle-to-vehicle communication network, while the physical element includes physical vehicle dynamics and human-driver responses. Within CAVN, communication networks enable opportunities for greater situational awareness, collaborative decision making, and improved control.

CAVNs have attracted considerable attention. From the cyber perspective, one significant challenge is the presence of inter-vehicular communication delay that limits the accessibility to timely and accurate information necessary for real-time control and accurate decision-making, see for example [2]. In general, one may classify the communication delays into two categories: naturally occurring, or adversarially induced. Naturally occurring communication delays are inherent to the cyber or physical components of the system. They could be random delays (latency) in the vehicle to vehicle (V2V) infrastructure or they could even model processing delays in the technology stack incurred from synchronizing data from multiple sensors, or physical latency in the CAN bus.

The wireless information communication of V2V uses short-to-medium range communication. CAVN platoons can use the Dedicated Short Range Communications for Wireless Access in Vehicular Environments (DSRC-WAVE) as in [3], [4]. Wireless access communication in vehicular environments covers up to 1 km in range with a rate of data transmission that is up to 27 Mbps, 5.9 GHz frequency, and a 75 MHz channel bandwidth. If the distance between two consecutive vehicles is less than 1 km then these vehicles are considered to be in the same platoon. That is, all vehicles within the same V2V wireless communications range are considered to be in the same platoon.

Recent studies consider non-ideal V2V communication time delays within the CAVN. It has been shown that these time lags in communication affect the system dynamics and degrade the performance of the CAVN, see, e.g., [5]. This includes the case of increasing communication time delay as the distance between the vehicles increases, and this issue can be considered as one of the worst scenarios in V2V communication delays [6]. In [6] a leader following control architecture is proposed to obtain string stability considering broadcast delays. In [5], a robust control of heterogeneous vehicular platoon with non-ideal communication is presented to compensate for the effect of the information delay. In [7], an adaptive control approach is proposed to solve the collaborative driving problem in the presence of non-ideal V2V communication. In [8], the authors study the stability of the equilibrium flow dynamics of CAVN with sensing, communication and human reaction delays. The study considers the number of vehicles as well as penetration rates of sensors and communication lines. In [9], a linear quadratic regulation is used to obtain an optimal design of connected cruise control with communication delay and driver reaction time.

In this work, we study the dynamics of CAVN with time delays under the assumption that communication time delays among vehicles increase as the distance between the vehicles increases. The paper is organized as follows. Section II provides a regular car platoon with commensurate delays between the communication links. In Section III, we provide plant stability analysis and characterize the maximum range of delay where the system becomes plant stable. In IV, we carry out string stability analysis. Section V presents the simulation results. Section VI concludes the paper.

II. The Model

Consider $n+1$ vehicles in single-lane road and let $i = 0, 1, \ldots, n$. The index $i = 0$ represents the leading vehicle and n is the total number of the following vehicles. We

I. Al-Darabsah and S. A. Campbell are with the Department of Applied Mathematics at University of Waterloo, Waterloo, ON, N2L 3G1, Canada Email: ialdarabsah@gmail.com, sacampbell@uwaterloo.ca.

M. Al Janaideh is with the department of Mechanical Engineering, Memorial University, St. John's, NL, Canada. Email: maljanaideh@mun.ca.

consider a control system model for a regular car platoon with commensurate delays of the form

$$\begin{bmatrix} \dot{s}_i(t) \\ \dot{v}_i(t) \end{bmatrix} = \begin{bmatrix} 0 & 1 \\ 0 & 0 \end{bmatrix} \begin{bmatrix} s_i(t) \\ v_i(t) \end{bmatrix} + \begin{bmatrix} 0 \\ 1 \end{bmatrix} u_i(t), \quad (1)$$

where the states s_i and v_i are the corresponding vehicle position and velocity, respectively, and u_i is control input that drives the vehicle i. The control signal can be written as [10]

$$u_i(t) = \sum_{j=0}^{i-1} [\alpha(\mathcal{V}(h_{i,j}(t-\zeta_{i,j})) - v_i(t-\zeta_{i,j})) \\ +\beta(v_j(t-\zeta_{i,j}) - v_i(t-\zeta_{i,j}))], \quad (2)$$

where $\alpha \in \mathbb{R}$ and $\beta \in \mathbb{R}$ are control gains, and $\zeta_{i,j}$ represents the communication time delay for data transferred from vehicle $j \in \{0, \ldots, i-1\}$ to i such that

$$\zeta_{i,i-1} < \ldots \zeta_{i,1} < \zeta_{i,0}. \quad (3)$$

Here the index $j = 0, 1, \ldots, i-1$ enumerates the vehicles in front of vehicle i. The time delays $\zeta_{i,j}$ indicate that communication time delays increase as the distance between the vehicles increases. The function $\mathcal{V} : \mathbb{R} \to \mathbb{R}$ is a range policy function that maps a distance to a velocity, and $h_{i,j}(t)$ represents the distance between the vehicles accounting for the length l_k of the k-th vehicle

$$h_{i,j}(t) = \frac{1}{i-j}(s_j(t) - s_i(t) - \sum_{k=j}^{i-1} l_k). \quad (4)$$

The continuous and smooth range policy function can be expressed as

$$\mathcal{V}(h) = \begin{cases} 0 & h \le h_{\mathrm{st}} \\ \frac{v_{\max}}{2}[1 - \cos(\frac{m\pi(h-h_{\mathrm{st}})}{h_{\mathrm{go}}-h_{\mathrm{st}}})] & h_{\mathrm{st}} < h < h_{\mathrm{go}} \\ v_{\max} & h \ge h_{\mathrm{go}} \end{cases}. \quad (5)$$

where h_{st}, h_{go} and $v_{\max}$ are positive constants. The parameter $m \in \mathbb{Z}^+$ and has the default value $m = 1$. The function $\mathcal{V}$ implies that the vehicle tends to stop for small distances $h \le h_{\mathrm{st}}$ and aims to maintain the preset maximum speed $v_{\max}$ for large distances $h \ge h_{\mathrm{go}}$. In the middle range, $h_{\mathrm{st}} < h < h_{\mathrm{go}}$, the desired velocity is determined by the specific function given by cosine.

In the literature, platooning cars are said to be in *uniform flow equilibrium* when each car moves at a constant velocity of v^* with constant headway h^*. In this scenario, it follows from (1) that

$$s_i^* = v^*t - ih^* - \sum_{k=0}^{i-1} l_k \quad \text{and} \quad \mathcal{V}(h^*) = v^*. \quad (6)$$

Notice that flow equilibrium is independent of time delays, the platoon size and control gains.

In this work, we study the plant stability and string stability of the linear system corresponding to the flow equilibrium in a special case of time delays when $\zeta_{i,j}$ is the $i-j$ multiple of a positive constant ϵ.

III. Stability Analysis

In this section, we study the *plant stability* of the linear system about the flow equilibrium in the presence of *commensurate delays*. We also characterize the maximal admissible delay region such that the time-delayed system remains stable. A vehicle network is said to be plant stable when the leading vehicle moves with a constant speed, and perturbations in the states of following vehicles approach to zero [11]. Two delays are said to be commensurate if their ratio is a rational number. Otherwise, they are incommensurate [12]. In the rest of the manuscript, we approximate the time delays as commensurate time delays of the form

$$\zeta_{i,j} = (i-j)\epsilon$$

for some constant $\epsilon > 0$, see Fig. 1.

Define the perturbations about the flow equilibrium as $\tilde{\mathbf{X}}_i := [\tilde{s}_i(t), \tilde{v}_i(t)]^T = [s_i(t), v_i(t)]^T - [s_i^*, v^*]^T$. Then, substituting $\tilde{\mathbf{X}}_i$ in (1) leads to

$$\dot{\tilde{\mathbf{X}}}_i(t) = \mathbf{A}_0\tilde{\mathbf{X}}_i(t) \\ + \sum_{j=0}^{i-1} \Big(\mathbf{A}_{i,j}\tilde{\mathbf{X}}_i(t-(i-j)\epsilon) + \mathbf{B}_{i,j}\tilde{\mathbf{X}}_j(t-(i-j)\epsilon) \Big), \quad (7)$$

where

$$\mathbf{A}_0 = \begin{bmatrix} 0 & 1 \\ 0 & 0 \end{bmatrix}, \ \mathbf{A}_{i,j} = \begin{bmatrix} 0 & 0 \\ -\psi_{i,j} & -\gamma \end{bmatrix}, \ \mathbf{B}_{i,j} = \begin{bmatrix} 0 & 0 \\ \psi_{i,j} & \beta \end{bmatrix} \quad (8)$$

with

$$\psi_{i,j} = \frac{\alpha\mathcal{V}'(h^*)}{i-j} \quad \text{and} \quad \gamma = \alpha + \beta. \quad (9)$$

Here $\mathcal{V}'$ is the first derivative of the range policy $\mathcal{V}$ with respect to h.

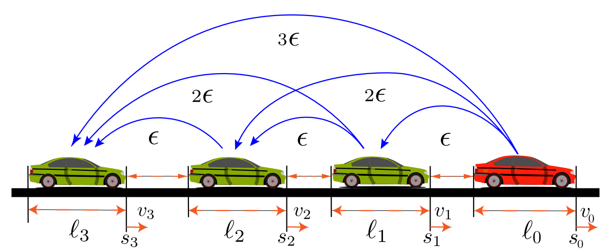

Fig. 1. Schematic representation of vehicles in the model (1) with $n = 3$ when $\zeta_{i,j} = (i-j)\epsilon$ for some $\epsilon > 0$. Here the car in red is the lead car (index 0). The blue arrows represent the flow of information which is subjected to delays $k\epsilon$, $k = 1, 2, 3$.

For the plant stability, we take $\tilde{v}_0 \equiv 0$ and seek $\tilde{v}_i(t) \to 0$ as $t \to \infty$ for $i = 1, \ldots, n$ [11]. This is equivalent to proving that the zero solution of (7) is stable, that is, the real part of all eigenvalues of the characteristic equation is negative. Let $\mathbf{X}(t) = [\tilde{\mathbf{X}}_1(t), \cdots, \tilde{\mathbf{X}}_n(t)]^T$. Then, (7) can be written as

$$\dot{\mathbf{X}}(t) = \mathbf{H}_0\mathbf{X}(t) + \sum_{k=1}^{n-1} \mathbf{H}_k\mathbf{X}(t-k\epsilon), \quad (10)$$

where

$$\mathbf{H}_0 = \mathrm{diag}\left(\mathbf{A}_0, \mathbf{A}_0, \ldots, \mathbf{A}_0\right),$$

and

$$\mathbf{H}_k = \mathrm{diag}\left(0,\ldots,0,\mathbf{A}_{i,i-k},\mathbf{A}_{i+1,i-k+1},\ldots,\mathbf{A}_{n,n-k}\right)\big|_{i>k} + \mathrm{Block}\big(\mathbf{B}_{i,j}\big)\big|_{i-j=k}.$$

The stability of (10) is determined by the eigenvalues of its corresponding characteristic equation. To find the characteristic equation, let

$$\mathbf{X}(t) = \mathbf{c}\mathrm{e}^{st},\ s\in\mathbb{R},\ \mathbf{c}\in\mathbb{R}^n. \tag{11}$$

Then, the characteristic equation associated with (10) has the form

$$\Delta(s;\epsilon) := \det\left(s\mathbf{I}_{2n} - \mathbf{H}_0 - \sum_{k=1}^{n-1}\mathbf{H}_k\mathrm{e}^{-k\epsilon s}\right) = 0. \tag{12}$$

The zero solution of (10) is stable if and only if

$$\hat{s} := \max\left\{\mathrm{Re}\,(s) : \Delta(s;\epsilon) = 0\right\} < 0.$$

The number $\hat{s}$ is called the *stability exponent* (the maximum of Lyapunov exponents) of the system (10).

To construct the maximal admissible delay region such that the time-delayed system remains stable, first, we study the stability when $\epsilon = 0$. By [13, Proposition 2.7.1], we obtain that

$$\begin{aligned}\Delta(s;0) &= \prod_{i=1}^{n}\begin{vmatrix} s & -1 \\ \sum_{j=1}^{i-1}\psi_{i,j} & s+(i-1)\gamma \end{vmatrix} \\ &= \prod_{i=1}^{n}\left(s^2+(i-1)\gamma s+\sum_{j=0}^{i-1}\psi_{i,j}\right).\end{aligned} \tag{13}$$

For $i = 1,\ldots,n$, denote

$$\Psi_i = \sum_{j=0}^{i-1}\psi_{i,j}.$$

Then the Routh-Hurwitz stability criterion [14] implies that the roots of (13) have negative real parts if and only if $\gamma > 0$ and $\Psi_i > 0$ for all $i = 1,\ldots,n$.

Lemma 3.1: When $\epsilon = 0$, the zero solution of (10) is stable if and only if

$$\gamma > 0 \quad \text{and} \quad \Psi_i > 0 \tag{14}$$

for all $i = 1,\ldots,n$.

When $\epsilon > 0$, we use the frequency-sweeping tests to obtain stability criteria [12]. Based on the continuity property of the stability exponent with respect to delays [12], in the following, we use the frequency-sweeping tests to to determine whether the stability exponent intersects the imaginary axis (existences of $s = I\omega$, $I = \sqrt{-1}$, in (12)) for $\epsilon > 0$ provided the zero solution of (10) is stable when $\epsilon = 0$. The idea is to replace the eigenvalues of

$$\bar{\Delta}(\omega) := \det\left(I\omega\mathbf{I}_{2n} - \mathbf{H}_0 - \sum_{k=1}^{n-1}\mathbf{H}_k\mathrm{e}^{-kI\omega\epsilon}\right) \tag{15}$$

by the *generalized eigenvalues* of a matrix pair $(\mathbf{P}(I\omega),\mathbf{Q}(I\omega))$ for some matrices $\mathbf{P}$ and $\mathbf{Q}$.

Definition 3.1 ([15]): $\lambda := \lambda(\mathbf{P},\mathbf{Q}) \in \mathbb{C}$ is a generalized eigenvalue of the matrix pair $(\mathbf{P},\mathbf{Q})$ if and only if $\det(\mathbf{P}-\lambda\mathbf{Q}) = 0$. The minimum $|\lambda|$ is denoted by

$$\rho(\mathbf{P},\mathbf{Q}) = \min\left\{|\lambda| : \det(\mathbf{P}-\lambda\mathbf{Q}) = 0\right\}. \tag{16}$$

Remark 3.1: The number of finite generalized eigenvalues for the matrix pair $(\mathbf{P},\mathbf{Q})$ is at most equal to the rank of $\mathbf{Q}$. Also, $\lambda(\mathbf{P},\mathbf{Q})$ is continuous with respect to the elements of $\mathbf{P}$ and $\mathbf{Q}$ when the rank of $\mathbf{Q}$ is constant [15].

First, we give the following matrix identity, which is a consequence of Schur's complement for determinants [16].

Lemma 3.2 ([12]): For any $z\in\mathbb{C}$ and matrices $\mathbf{W}_k \in \mathbb{C}^{m\times m}$, $k = 0,1,\ldots,n-1$,

$$\det\left(\sum_{k=0}^{n-1}\mathbf{W}_k z^k\right) = \det\left\{ z\begin{pmatrix} \mathbf{I}_{2n} & 0 & \cdots & 0 \\ 0 & \ddots & \ddots & \vdots \\ \vdots & \vdots & \mathbf{I}_{2n} & 0 \\ 0 & 0 & \cdots & \mathbf{W}_{n-1}\end{pmatrix} - \begin{pmatrix} 0 & \mathbf{I}_{2n} & \cdots & 0 \\ \vdots & \vdots & \ddots & \vdots \\ 0 & 0 & \cdots & \mathbf{I}_{2n} \\ -\mathbf{W}_0 & -\mathbf{W}_1 & \cdots & -\mathbf{W}_{n-2}\end{pmatrix}\right\}. \tag{17}$$

Now, let $z = \mathrm{e}^{-I\omega\epsilon}$, $\mathbf{W}_0 = I\omega\mathbf{I}_{2n} - \mathbf{H}_0$ and $\mathbf{W}_k = -\mathbf{H}_k$ in (15). Notice that the size of $\mathbf{H}_k$ is $2n$. Then by Lemma 3.2, we have

$$\begin{aligned}\bar{\Delta}(\omega) &= (-1)^{2(n-1)}\det\Big(\mathbf{P}(I\omega) - \mathrm{e}^{-I\omega\epsilon}\mathbf{Q}\Big) \\ &= \det\Big(\mathbf{P}(I\omega) - \mathrm{e}^{-I\omega\epsilon}\mathbf{Q}\Big)\end{aligned} \tag{18}$$

where

$$\mathbf{P}(s) := \begin{pmatrix} 0 & \mathbf{I}_{2n} & \cdots & 0 \\ \vdots & \vdots & \ddots & \vdots \\ 0 & 0 & \cdots & \mathbf{I}_{2n} \\ -(s\mathbf{I}_{2n}-\mathbf{H}_0) & \mathbf{H}_1 & \cdots & \mathbf{H}_{n-2}\end{pmatrix} \tag{19}$$

and

$$\mathbf{Q} := \mathrm{diag}\left(\mathbf{I}_{2n},\ldots,\mathbf{I}_{2n},-\mathbf{H}_{n-1}\right). \tag{20}$$

The following result characterizes the maximum range of delay where the system becomes plant stable.

Theorem 3.1: Let $\mathrm{rank}(\mathbf{H}_{n-1}) = r$ and assume that condition (14) is satisfied, that is, the zero solution of (10) is stable when $\epsilon = 0$. Furthermore, for $i \in \{1,\ldots,r+2n(n-2)\}$, define

$$\bar{\epsilon}_i = \begin{cases} \min\limits_{1\le k\le n-1}\frac{\theta_k^i}{\omega_k^i} & \text{if } \lambda_i(\mathbf{P}(I\omega_k^i),\mathbf{Q}) = \mathrm{e}^{-I\theta_k^i} \\ & \text{for some } \omega_k^i\in(0,\infty), \theta_k^i\in[0,2\pi], \\ \infty & \text{if } \rho(\mathbf{P}(I\omega),\mathbf{Q}) > 1, \forall\omega\in(0,\infty). \end{cases} \tag{21}$$

Then, the zero solution remains stable for $\epsilon\in(0,\epsilon^*)$ where

$$\epsilon^* = \min\left\{\bar{\epsilon}_i : 1\le i\le r+2n(n-2)\right\}. \tag{22}$$

Proof: To show that the stability exponent is negative, there are two cases for ϵ^*:

Case 1: $\epsilon^* < \infty$. Since $\mathrm{rank}(\mathbf{H}_{n-1}) = r$, we have $\mathrm{rank}(\mathbf{Q}) = r + 2n(n-1)$. Thus, there are at most $r + 2n(n-1)$ generalized eigenvalues λ_i for the matrix pair

$(\mathbf{P}(I\omega), \mathbf{Q})$, see Remark 3.1.

Let $\epsilon \in [0, \epsilon^*)$ and $\omega \in (0, \infty)$. When $\omega = \omega_k^i$, then by (21), we get $\epsilon\omega_k^i \neq \theta_k^i$ and

$$\det\left(\mathbf{P}(I\omega_k^i) - \mathrm{e}^{-I\theta_k^i}\mathbf{Q}\right) = 0. \tag{23}$$

Hence,

$$\det\left(\mathbf{P}(I\omega_k^i) - \mathrm{e}^{-I\omega_k^i\epsilon}\mathbf{Q}\right) \neq 0. \tag{24}$$

When $\omega \neq \omega_k^i$, then by (21) we have $\lambda_i(\mathbf{P}(I\omega), \mathbf{Q}) \neq \mathrm{e}^{-I\theta_k^i}$. Thus, $|\lambda_i(\mathbf{P}(I\omega), \mathbf{Q})| \neq 1$. Hence, by Definition 3.1, we have

$$\det\left(\mathbf{P}(I\omega) - \mathrm{e}^{-I\omega\epsilon}\mathbf{Q}\right) \neq 0. \tag{25}$$

Thus, the equation $\bar{\Delta}(\omega) = 0$ does not have any eigenvalue for $\epsilon \in [0, \epsilon^*)$. Since the zero solution is stable at $\epsilon = 0$, the continuity argument of the stability exponent implies that it remains stable for all $\epsilon \in [0, \epsilon^*)$.

At $\epsilon = \epsilon^*$, there exists a pair (ω_k^i, θ_k^i) such that $\epsilon^*\omega_k^i = \theta_k^i$ and $\lambda_i(\mathbf{P}(I\omega_k^i), \mathbf{Q}) = \mathrm{e}^{-I\theta_k^i}$. Thus,

$$\det\left(\mathbf{P}(I\omega_k^i) - \mathrm{e}^{-I\theta_k^i}\mathbf{Q}\right) = \det\left(\mathbf{P}(I\omega_k^i) - \mathrm{e}^{-I\epsilon^*\omega_k^i}\mathbf{Q}\right) = 0.$$

Thus, an eigenvalue of $\bar{\Delta}(\omega) = 0$ intersects the imaginary axis at $\epsilon = \epsilon^*$.

Case 2: For the case when $\epsilon^* = \infty$, first, we prove the following claim.

*C*laim. For $\omega > 0$ and $\epsilon > 0$, we have

$$\rho(\mathbf{P}, \mathbf{Q}) = \rho\left(\mathbf{P}, \mathbf{Q}\mathrm{e}^{-\epsilon I\omega}\right). \tag{26}$$

Let $\lambda \in \mathbb{C}$. Then, there exists $\hat{\lambda}$ such that $\lambda = \hat{\lambda}\mathrm{e}^{-\epsilon I\omega}$ and $|\lambda| = \left|\hat{\lambda}\right|$. Indeed, multiplying $\hat{\lambda}$ by $\mathrm{e}^{-\epsilon I\omega}$ will rotate it around the origin in the complex plane without changing its magnitude. Consequently, we have

$$\begin{aligned}\rho(\mathbf{P}, \mathbf{Q}) &= \min\left\{|\lambda| : \det(\mathbf{P} - \lambda\mathbf{Q}) = 0\right\} \\ &= \min\left\{\left|\hat{\lambda}\mathrm{e}^{-\epsilon I\omega}\right| : \det(\mathbf{P} - \hat{\lambda}\mathrm{e}^{-\epsilon I\omega}\mathbf{Q}) = 0\right\} \\ &= \min\left\{\left|\hat{\lambda}\right| : \det(\mathbf{P} - \hat{\lambda}\mathrm{e}^{-\epsilon I\omega}\mathbf{Q}) = 0\right\} \\ &= \rho(\mathbf{P}, \mathbf{Q}\mathrm{e}^{-\epsilon I\omega}).\end{aligned}$$

Now, by (21) and (22), $\epsilon^* = \infty$ holds when $\rho(\mathbf{P}(I\omega), \mathbf{Q}) > 1,\ \forall\omega \in (0, \infty)$. Then by (26), we get

$$\rho\left(\mathbf{P}(I\omega), \mathbf{Q}\mathrm{e}^{-\epsilon I\omega}\right) > 1 \tag{27}$$

for any $\omega > 0$ and $\epsilon > 0$. Hence, for any $\epsilon > 0$, we obtain

$$\det\left(\mathbf{P}(I\omega) - \mathrm{e}^{-I\omega\epsilon}\mathbf{Q}\right) \neq 0 \quad \forall\omega \in (0, \infty). \tag{28}$$

Hence, no eigenvalue satisfies $\bar{\Delta}(\omega) = 0$ for all $\epsilon > 0$. Since the zero solution is stable at $\epsilon = 0$ and due to the continuity of the stability exponent, we have

$$\det\left(\mathbf{P}(s) - \mathrm{e}^{-s\epsilon}\mathbf{Q}\right) \neq 0 \quad \forall s \in \bar{\mathbb{C}}_+ \tag{29}$$

for any $\epsilon > 0$. Here, $\bar{\mathbb{C}}_+$ in the closed right half plane. Hence, the zero solution is stable for all $\epsilon \in [0, \infty)$. In this case, the zero solution is stable independent of delay [12]. This completes the proof. ∎

Theorem 3.1 implies that all eigenvalues of (12) are negative when $\epsilon \in (0, \epsilon^*)$, thus the exponential term in (11) will go to zero as $t \to \infty$. Hence, $\tilde{\mathbf{X}}_i$ converges toward zero, that is, the system is plant stable.

When the matrix $\mathbf{P}(I\omega)$ is nonsingular, we have

$$\rho(\mathbf{P}(I\omega), \mathbf{Q}) = \frac{1}{\sigma(\mathbf{P}^{-1}(I\omega)\mathbf{Q})} \tag{30}$$

where σ is the spectral radius of a matrix. The inverse of the matrix $\mathbf{P}(I\omega)$ is given by

$$\mathbf{P}^{-1}(I\omega) = \begin{pmatrix} (I\omega\mathbf{I}_{2n} - \mathbf{H_0})^{-1}\mathbf{H}_1 & \cdots & (I\omega\mathbf{I}_{2n} - \mathbf{H_0})^{-1}\mathbf{H}_{n-2} & -(I\omega\mathbf{I}_{2n} - \mathbf{H_0})^{-1} \\ \mathbf{I}_{2n} & \cdots & 0 & 0 \\ \vdots & \ddots & \vdots & \vdots \\ 0 & \cdots & \mathbf{I}_{2n} & 0 \end{pmatrix}.$$

Hence, when $\mathbf{P}(I\omega)$ is invertible, we obtain

$$\mathrm{Sign}\Big(\rho(\mathbf{P}(I\omega), \mathbf{Q}) - 1\Big) = \mathrm{Sign}\Big(1 - \sigma(\mathbf{P}^{-1}(I\omega)\mathbf{Q})\Big). \tag{31}$$

Consequently, we can use (31) to check whether or not the zero solution is stable independent of delay.

IV. String Stability

In this section, we study the string stability of (7) in the presence of time delays. This is critical in the dynamics of the vehicle network to avoid amplifying spacing errors downstream of the traffic flow [17]. The string instability of a platoon can cause the emergence of a jam, such as stop and go, in circuits and single-lane roads. Through this section, we assume (7) is plant stable, that is, $\epsilon \in (0, \epsilon^*)$.

The velocity $\tilde{v}_i(t)$ in (7) can be written $\tilde{v}_i(t) = \mathbf{C}\tilde{\mathbf{X}}_i(t)$ with $\mathbf{C} = [0, 1]$. Let $V_i(\xi)$ be the Laplace transform of $\tilde{v}_i(t)$ and assume zero initial conditions. Then, from (7) we have

$$V_i(\xi) = \sum_{j=0}^{i-1} G_{i,j}(\xi)V_j(\xi) \tag{32}$$

where

$$G_{i,j}(\xi) = \mathrm{e}^{-(i-j)\epsilon\xi}\mathbf{C}\times \left(\xi\mathbf{I}_2 - \mathbf{A}_0 - \sum_{j=0}^{i-1}\mathrm{e}^{-(i-j)\epsilon\xi}\mathbf{A}_{i,j}\right)^{-1}\mathbf{B}_{i,j}\mathbf{E}(\xi). \tag{33}$$

Here $\mathbf{I}_2$ is the identity matrix of size 2 and $\mathbf{E}(\xi) = [\xi^{-1}, 1]^T$ that satisfies $\mathbf{Y}_i(\xi) = \mathbf{E}(\xi)V_i(\xi)$ where $\mathbf{Y}_i(\xi)$ is the Laplace transform of the state $\tilde{\mathbf{X}}_i(t)$ in (7). The function $G_{i,j}$ is called the *link transfer function* which acts as a dynamic weight along the link between vehicles i and j [18]. Consequently, by substituting (8) in (33), we write $G_{i,j}$ as

$$G_{i,j}(\xi) = \frac{(\beta\xi + \psi_{i,j})\,\mathrm{e}^{-(i-j)\epsilon\xi}}{\xi^2 + \sum_{k=0}^{i-1}(\gamma\xi + \psi_{i,k})\,\mathrm{e}^{-(i-k)\epsilon\xi}}. \tag{34}$$

To describe the dynamic relationship between any two vehicles i and j, we can obtain the transfer function $T_{i,j}$ from (32) such that

$$V_i(\xi) = T_{i,j}(\xi)V_j(\xi) \tag{35}$$

which contains the dynamics of all vehicles between vehicles i and j. Since we have the same connection topology as in [19] for system (1), we know that the string stability can be obtained by only considering $T_{n,0}(\xi)$, that is, the system is string stable if and only if

$$\sup_{\omega>0} |T_{n,0}(I\omega)| < 1. \tag{36}$$

To find $T_{n,0}(\xi)$, define the matrix

$$\mathbf{G}(\xi) := \Big[G_{i+1,j+1}(\xi)\Big]_{j=0,\ldots,i-1}^{i=0,\ldots,n}. \tag{37}$$

Notice that $\mathbf{G}(\xi) \in \mathbb{C}^{(n+1)\times(n+1)}$. Then, $T_{n,0}(\xi)$ given by the bottom-left elements of the matrix

$$\mathbf{T}(\xi) = \sum_{k=1}^{n} (\mathbf{G}(\xi))^k. \tag{38}$$

For the details on the mathematical derivation, see [19].

V. Numerical Results

In this section, we use the range policy described in (5) with : $m = 1$, $h_{\text{st}} = 0.1m$, $h_{\text{go}} = 2.2m$, and $v_{\max} = 0.25m/s$. When $\alpha = 0.8$, $\beta = 0.2$ and $h^* = 1$, then $\mathcal{V}'(h^*) = 0.182$, $\gamma = 1$, $\Psi_1 = 0.146$, $\Psi_2 = 0.218$, $\Psi_3 = 0.267$ and $\Psi_3 = 0.303$. Hence, system (7) is plant stable (speed errors converge toward zero) when there is no delay $\epsilon = 0$ as given in Lemma 3.1, see Fig. 2.

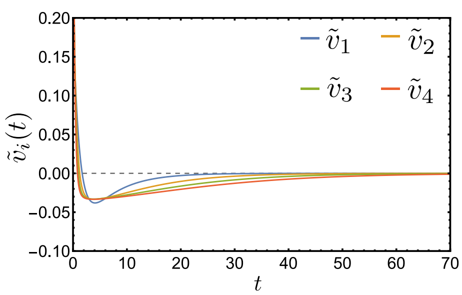

Fig. 2. Time series of $\tilde{v}_i(t)$ of system (7) with $\epsilon = 0$ and $n = 4$. As per Lemma 3.1, system (7) is plant stable when $\gamma > 0$ and $\Psi_i > 0$ for $i = 1, 2, 3, 4$.

Next, we check whether the zero solution is stable independent of delay or not. Fig. 3 shows the spectral radius σ of the matrix $\mathbf{P}^{-1}(I\omega)\mathbf{Q}$. We notice that $\sigma < 1$ for some $\omega \in (0, \infty)$. Hence, from (31), we have $\rho(\mathbf{P}(I\omega), \mathbf{Q}) > 1$ does not hold for all $\omega \in (0, \infty)$ in Theorem 3.1. Therefore, it follows from Theorem 3.1 that the stability of the zero solution depends on the time delay.

Now we calculate the critical frequency-angle pairs (ω_k^i, θ_k^i) by finding ω for which $|\lambda_i(\mathbf{P}(I\omega), \mathbf{Q})|$ cross the value of 1. In Fig. 4, we find 10 generalised eigenvalues and observe that $|\lambda_1|$, $|\lambda_2|$, $|\lambda_6|$ and $|\lambda_8|$ cross the horizontal line

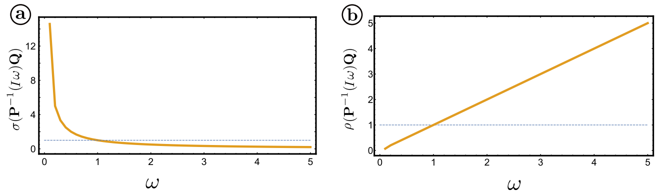

Fig. 3. (a) $\sigma(\mathbf{P}^{-1}(I\omega)\mathbf{Q})$: the spectral radius of matrix $\mathbf{P}^{-1}(I\omega)\mathbf{Q}$. (b) The value of ρ as defined in (16). As we can see the graphs of σ and ρ are consistent with (31). Both σ and ρ cross the value of 1 at one point, hence, the stability of the zero solution in (7) depends on the time delay.

of magnitude 1 at $\omega_1^1 = 1.0103$, $\omega_1^2 = 1.7751$, $\omega_1^6 = 2.4675$ and $\omega_1^8 = 3.1338$. Consequently , we have

$$\lambda_1 = 0.1429 - 0.9897I = \mathrm{e}^{-1.4274I},$$
$$\lambda_2 = 0.5347 - 0.8450I = \mathrm{e}^{-1.0066I},$$
$$\lambda_6 = 0.7194 - 0.6946I = \mathrm{e}^{-0.7679I},$$
$$\lambda_8 = 0.8144 - 0.5803I = \mathrm{e}^{-0.6192I}.$$

This yields the critical frequency-angle pairs (ω_1^i, θ_1^i):

$$(1.0103, 1.4274), \quad (1.7751, 1.0066),$$
$$(2.4675, 0.7679), \quad (3.1338, 0.6192).$$

Thus, from Theorem 3.1, we have

$$\epsilon^* = \min_{i\in\{1,2,6,8\}} \left\{\frac{\theta_1^i}{\omega_1^i}\right\} = 0.1976.$$

As per Theorem 3.1, system (7) is plant stable when $\epsilon < \epsilon^*$ and plant unstable when $\epsilon > \epsilon^*$, see Figs. 5-6. In Fig. 7, we fix ϵ and plot the stability region in (α, β) plane, we notice that the stability region of the zero solution in (7) becomes smaller as the time delay ϵ increases. When ϵ becomes larger, there will be less choices for the control gains to stabilize the system (7).

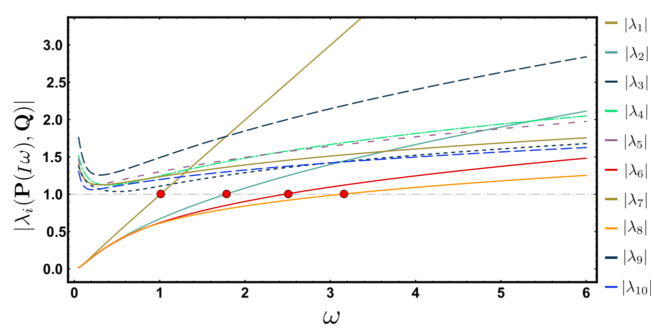

Fig. 4. The magnitude of the generalized eigenvalue λ_i of the matrix pair $(\mathbf{P}(I\omega), \mathbf{Q})$, $i = 1, \ldots, 10$. The curve of $|\lambda_1|$, $|\lambda_2|$, $|\lambda_6|$ and $|\lambda_8|$ crosses the horizontal line of magnitude 1.

For the string stability, we use (38) to find the transfer function

$$\begin{aligned} T_{4,0}(\xi) = {} & G_{4,0}(\xi) + G_{4,1}(\xi)G_{1,0}(\xi) + G_{4,2}(\xi)\,(G_{2,1}(\xi) \\ & G_{1,0}(\xi) + G_{2,0}(\xi)) + G_{4,3}(\xi)\,(G_{3,0}(\xi) + G_{3,1}(\xi) \\ & G_{1,0}(\xi) + G_{3,2}(\xi)\,[G_{2,1}(\xi)G_{1,0}(\xi) + G_{2,0}(\xi)]) \end{aligned}$$

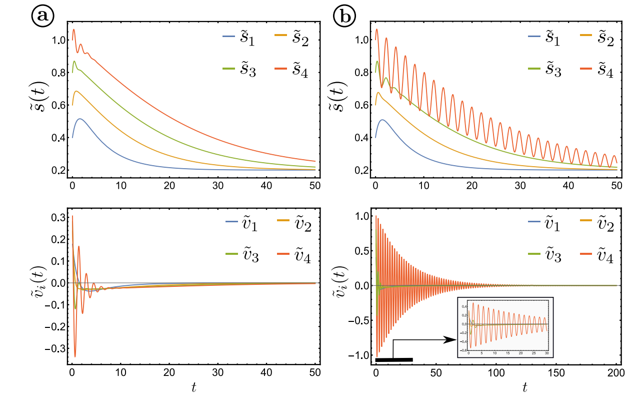

Fig. 5. Time series of $\tilde{s}_i(t)$ and $\tilde{v}_i(t)$ of system (7) with $n = 4$. The solution $\tilde{v}_i(t)$ converges toward zero, that is, system (7) is plant stable when $\epsilon < \epsilon^*$ as per Theorem 3.1 (a) $\epsilon = 0.12$ (b) $\epsilon = 0.19$.

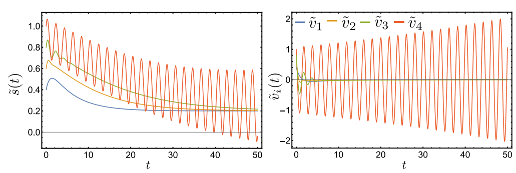

Fig. 6. Time series of $\tilde{s}_i(t)$ and $\tilde{v}_i(t)$ of system (7) with $n = 4$. System (7) is plant unstable when $\epsilon = 0.21 > \epsilon^*$ as per Theorem 3.1.

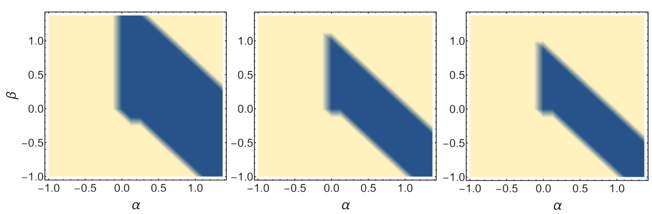

(a) $\epsilon = 0.12$ (b) $\epsilon = 0.19$ (c) $\epsilon = 0.21$

Fig. 7. Stability charts in α and β plane for $(\alpha, \beta) \in [-1, 1.5] \times [-1, 1.5]$. The stability region is colored by blue. We notice that there will be more choices for the control gains to stabilize the system (7) for smaller ϵ.

where

$$G_{i,j}(\xi) = \frac{\left(0.2\xi + \frac{0.1456}{i-j}\right) e^{-(i-j)\epsilon\xi}}{\xi^2 + \sum_{k=0}^{i-1} \left(\frac{(i-k)\xi + 0.1456}{i-k}\right) e^{-(i-k)\epsilon\xi}}$$

As shown in Fig. 5, system (7) is plant stable when $\epsilon = 0.12, 0.19$. By studying the sup $|T_{4,0}(I\omega)|$ for $\omega > 1$, we can see in Fig. 8 that system (7) is string stable when $\epsilon = 0.12$ and string unstable when $\epsilon = 0.19$.

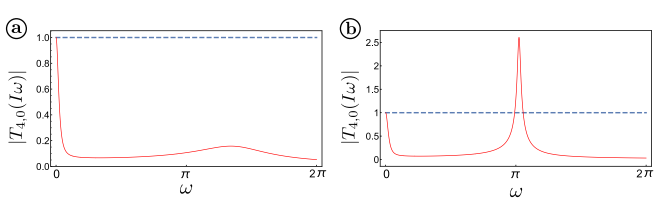

Fig. 8. The curve of $|T_{4,0}(I\omega)|$ when (a) $\epsilon = 0.12$ (b) $\epsilon = 0.19$. System (7) is string stable when $\epsilon = 0.12$ because the the maximum value of $|T_{4,0}(I\omega)|$ is less than 1 for all $\omega > 0$ and it is string unstable when $\epsilon = 0.19$ since the curve of $|T_{4,0}(I\omega)|$ is bigger than 1 for $\omega \in (0, \infty)$.

VI. Conclusions

We studied Connected Autonomous Vehicle Networks (CAVN) under the assumption that communication time delays increase as the distance between the vehicles increases. We assumed commensurate time delays in CAVN where the ratio of any two delays is a rational number. We carried out plant stability and string stability analysis and obtained the maximum range of delay where the CAVN becomes plant stable. We also observed that the stability region in the control gains plane becomes smaller as the time delays increase.

References

[1] A. Sarker, H. Shen, M. Rahman, M. Chowdhury, K. Dey, F. Li, Y. Wang, and H. S. Narman, "A review of sensing and communication, human factors, and controller aspects for information-aware connected and automated vehicles," *IEEE trans Intell Transp Syst*, vol. 21, no. 1, pp. 7–29, 2019.

[2] D. Wang and R. Sipahi, "Stability analysis of a large-scale single-lane connected vehicle model with multiple sensing, communication, and human reaction delays," *Proc Am Control Conf*, pp. 404–409., 2020.

[3] M. Pirani, E. Hashemi, A. Khajepour, B. Fidan, B. Litkouhi, S.-K. Chen, and S. Sundaram, "Cooperative vehicle speed fault diagnosis and correction," *IEEE trans Intell Transp Syst*, vol. 20, pp. 783–789, 2018.

[4] I. T. S. Committee, "IEEE standard for wireless access in vehicular environments (WAVE)-identifier allocations," IEEE, Tech. Rep., 2013.

[5] B. Liu, F. Gao, Y. He, and C. Wang, "Robust control of heterogeneous vehicular platoon with non-ideal communication," *Electronics*, vol. 8, pp. 1–16., 2019.

[6] A. A. Peters, R. H. Middleton, and O. Mason, "Leader tracking in homogeneous vehicle platoons with broadcast delays," *Automatica*, vol. 50, no. 1, pp. 64–74, 2014.

[7] A. Petrillo, A. Salvi, S. Santini, , and A. Valente, "Adaptive multi-agents synchronization for collaborative driving of autonomous vehicles with multiple communication delays," *Transp Res Part C Emerg Technol*, vol. 86, pp. 372–392., 2018.

[8] D. Wang and A. Rifat, "Stability analysis of a large-scale single-lane connected vehicle model with multiple sensing, communication and human reaction delays," *Proc Am Control Conf*, pp. 1–6, 2020.

[9] G. Jin and G. Orosz, "Optimal control of connected vehicle systems with communication delay and driver reaction time," *IEEE trans Intell Transp Syst*, pp. 2056–2070, 2017.

[10] R. Szalai and G. Orosz, "Decomposing the dynamics of heterogeneous delayed networks with applications to connected vehicle systems," *Phys Rev E*, vol. 88, no. 4, p. 040902, 2013.

[11] G. Orosz and S. P. Shah, "A nonlinear modeling framework for autonomous cruise control," in *Proc Dyn Sys and Contr Conf*, vol. 45301. American Society of Mechanical Engineers, 2012, pp. 467–471.

[12] K. Gu, J. Chen, and V. L. Kharitonov, *Stability of time-delay systems*. Springer Science & Business Media, 2003.

[13] D. S. Bernstein, *Matrix mathematics: theory, facts and formulas*. Princeton university press, 2009.

[14] W. S. Levine, *The Control Handbook (three volume set)*. CRC press, 2018.

[15] X.-D. Zhang, *Matrix analysis and applications*. Cambridge University Press, 2017.

[16] G. Golub and C. Van Loan, *Matrix Computations*. Johns Hopkins University Press, 2012.

[17] D. Swaroop and J. K. Hedrick, "String stability of interconnected systems," *IEEE Trans Automat Contr*, vol. 41, no. 3, pp. 349–357, 1996.

[18] D. Hajdu, L. Zhang, T. Insperger, and G. Orosz, "Robust stability analysis for connected vehicle systems," *IFAC-PapersOnLine*, vol. 49, no. 10, pp. 165–170, 2016.

[19] L. Zhang and G. Orosz, "Motif-based design for connected vehicle systems in presence of heterogeneous connectivity structures and time delays," *IEEE trans Intell Transp Syst*, vol. 17, no. 6, pp. 1638–1651, 2016.